Journal of Applied Mechanics and Technical Physics, Vol. 45, No. 3, pp. 335–343, 2004

EFFECT OF STREAMLINE CURVATURE ON INTENSITY OF STREAMWISE VORTICES IN THE MIXING LAYER OF SUPERSONIC JETS

V. I. Zapryagaev, N. P. Kiselev, and A. A. Pavlov

UDC 533.697

The structure of supersonic nonisobaric jets with Mach numbers $M_a = 1$ and 2 is considered experimentally to find the effect of streamline curvature on the evolution of streamwise vortices in the mixing layer. The spatial development of steady streamwise vortices in the mixing layer of supersonic jets is considered. A method for generation of steady streamwise vortices by applying microroughness elements of controlled size onto the inner surface of the nozzle is developed. Radial profiles and azimuthal variations of total pressure are obtained; the mixing-layer thickness and the curvature of streamlines in supersonic jets are determined. A significant effect of microroughnesselements of prescribed shape located on the nozzle surface on the behavior of total pressure in the mixing layer of supersonic jets, as compared to natural disturbances, is obtained.

Key words: *supersonic jet, nozzle, mixing layer, streamwise vortex structures, curvature of streamlines.*

The importance of studying a high-velocity jet mixing layer is caused by practical application of jets in injection systems for gaseous fuel, ejector systems for pressure recovery, and other devices where the mass transfer in the mixing layer plays the governing role [1, 2]. Effective methods for controlling mass-transfer processes by affecting the initial part of the mixing layer are currently sought [3]. A significant effect of streamwise vortex structures in the mixing layer on involvement of the external (relative to the jet) substance into turbulent mixing is noted [4].

Detailed investigations of formation and evolution of streamwise vortex structures in the mixing layer of a free nonisobaric supersonic jet exhausting into the ambient space at high Reynolds numbers has been started comparatively recently [5, 6]. The presence of azimuthal variations at the initial section of a supersonic underexpanded jet was revealed both in schlieren pictures, which display streamwise fringes, and by measuring the azimuthal distribution of total pressure in the flow. Azimuthal variations are manifested in jets exhausted from nozzles of different sizes with different gas-dynamic parameters, which indicates that this phenomenon is frequently encountered in jet flows. It was found [7–9] that roughness elements and local microroughnesses of the inner surface of the nozzle have a significant effect on formation of azimuthal inhomogeneities in the mixing layer of a high-velocity jet. The physical mechanism of evolution of streamwise vortices in the mixing layer is determined by processes described by the theory of hydrodynamic stability of the shear flow and also by additional factors caused by the curvature of streamlines at the boundary of a supersonic underexpanded jet.

A subsonic mixing layer in the presence of significant initial transverse disturbances introduced into the flow by a lobed mixer was studied in [10], where the formation and evolution of streamwise vortices in the subsonic mixing layer were analyzed in detail, and the vortex intensity was shown to rapidly decrease with distance from the source of generation of streamwise structures. Krothapalli et al. [11] made an attempt to determine which is the governing factor in the process of emergence of streamwise vortices in the mixing layer of a supersonic jet: roughness at the nozzle exit or curvature of streamlines. Krothapalli et al. [11] estimates the role of defects in nozzle manufacturing and argued that the curvature can lead to spatial amplification of three-dimensional disturbances in

Institute of Theoretical and Applied Mechanics, Siberian Division, Russian Academy of Sciences, Novosibirsk 630090. Translated from Prikladnaya Mekhanika i Tekhnicheskaya Fizika, Vol. 45, No. 3, pp. 32–43, May–June, 2004. Original article submitted June 5, 2003.

0021-8944/04/4503-0335

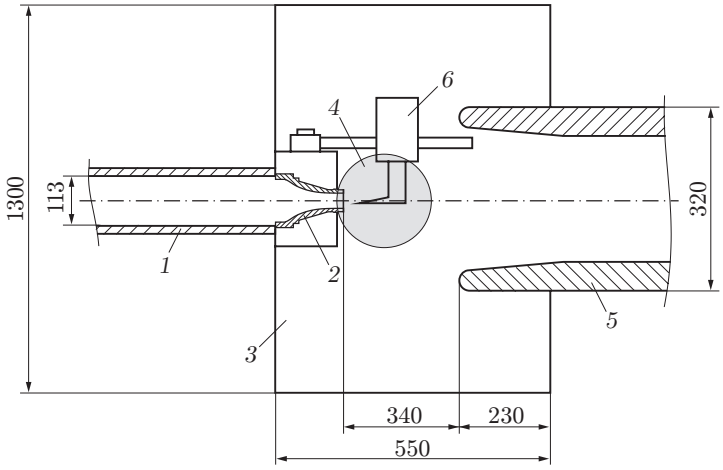

Fig. 1. Layout of the jet unit of the T-326 hypersonic blowdown wind tunnel: 1) plenum chamber of the jet unit; 2) replaceable nozzles; 3) test chamber; 4) window; 5) supersonic diffuser; 6) radial-azimuthal traversing gear.

the mixing layer of the jet, but this condition cannot substantially affect disturbance dynamics.

In experimental investigations [12, 13] of spatial development of steady streamwise vortices in the mixing layer of a supersonic jet, a nonmonotonic radial distribution of the amplitude of some spectral modes corresponding to streamwise structures of different scales was obtained. A complicated character of the Fourier distributions of amplitude as functions of the azimuthal wavenumber (a large number of peaks in the range of wavenumbers from 3 to 40) obtained by expansion of azimuthal dependences of total pressure in the mixing layer of the jet exhausting from a nozzle with natural roughness was noted.

The objective of the present work was to obtain quantitative data on the influence of streamline curvature in the mixing layer of the jet on evolution of steady streamwise disturbances. To minimize uncontrolled disturbances on the inner surface of the layer, new nozzles were fabricated with more perfect equipment. The main parameters affecting the development of steady streamwise vortices are the flow Mach number, curvature of streamlines, mixing-layer thickness, radial gradient of density, Reynolds number, and also the level and spectral composition of initial disturbances. A change in one parameter usually involves changes in other quantities characterizing the gas-dynamic mode of jet exhaustion. Therefore, conditions for determining streamwise curvature in the mixing layer were provided.

The experiments were performed in a jet unit of a T-326 hypersonic blowdown wind tunnel. The layout of the jet unit is shown in Fig. 1. The plenum chamber 1 of the jet unit is a tube with an inner diameter of 113 mm and with a seat for replaceable nozzles 2. The jet is exhausted into the test chamber 3 whose size is $1.3 \times 0.55 \times 0.93$ m. The nozzle exit is located in the field of vision of the optical window 4 with a diameter of 200 mm. The supersonic jet is exhausted into the pressure chamber and is ejected into the damping chamber through a supersonic diffuser 5 at the wind-tunnel outlet.

The pressure probes were moved by a radial-azimuthal traversing gear 6 fixed on the outer surface of the nozzle. The traversing gear ensured displacement of pressure probes (Pitot tubes or static pressure probes) in the radial direction r, over the azimuthal angle φ in the range of 0–360°, and along the jet centerline x. A Pitot tube with an outer diameter of 0.6 mm was used in the experiment. The accuracy of motion was 0.01 mm in the radial direction, 0.1 mm in the longitudinal direction, and 0.2° in terms of the azimuthal angle. The Pitot tube was moved along the coordinates r and φ by stepped motors and special gears free from slack. The traversing gear was controlled by a special control panel either manually or with the help of a special computer.

The data acquisition system is based on the use of a multifunctional PCI-1710HG board with a 12-digit analog-to-digital converter, produced by Advantech. The code for acquisition of experimental data allows one to control the traversing gear in an automatic mode and register the pressure in the plenum chamber (P_0) and in the test section of the wind tunnel (P_{ch}), as well as the pressure measured by the Pitot tube (P_t). In addition, the temperature in the plenum chamber of the jet unit (T_0) and the temperature in the test chamber (T_{ch}) were measured. The data acquisition code allows an increase in accuracy of the measured quantities by averaging multiple measurement results.

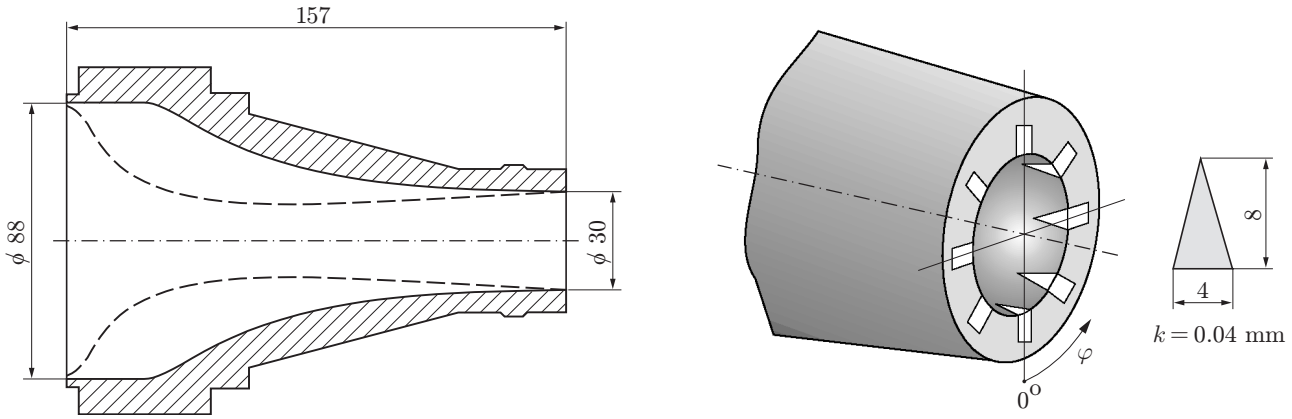

Fig. 2. Contoured nozzles for Mach numbers $M_a = 1$ (solid curves) and $M_a = 2$ (dashed curves) and positions of "microtabs" on the inner surface of the nozzle.

Two nozzles with geometric Mach numbers in the exit section $M_a = 1$ and 2 (Fig. 2) were used. The diameters of the input and output cross sections of both nozzles were identical and equal to $D_a = 30$ mm. The contour of the subsonic part of the nozzle was calculated by the Vitoshinskii formula [14].

Deviations of the inner surfaces of the nozzles from a regular circle were measured at a distance of 3 mm from the nozzle-exit section by a 73PC roundness-measurement instrument produced by Taylor Rank. For comparison, deviations from the circle were measured for previously used nozzles of diameter $D_a = 20$ mm [11, 12]. Deviations of the new nozzles are significantly smaller than those of nozzles used previously ($e \approx 2.65$ and ≈ 12 μm, respectively), which is explained by a higher quality of equipment used.

The surface roughness was measured by longitudinal displacement of the measurement tip near the nozzle-exit section by a 120L profilometer produced by Form Talysurf. The mean roughness of the surface of the nozzles used is approximately 5 times lower than that of the previously used nozzles. For instance, the roughness of the previously used nozzle of diameter $D_a = 20$ mm [in accordance with the Rz(ISO) standard] is approximately 2 μm, whereas a typical value of roughness for the new nozzles, which is determined as the mean height of roughness elements on the nozzle profile, is approximately 0.25 μm.

The relative roughness equal to the ratio of the roughness height to the boundary-layer displacement thickness at the nozzle exit is approximately 0.0005 for the new nozzles and 0.02 for the old ones. The decrease in relative roughness of the new nozzles can be attributed not only to the better quality of their surface but also to the increase in the boundary-layer thickness at the exit of the nozzles used in these studies. The relative boundary-layer thickness at the exit of the new nozzles is $\delta/R_a = 0.22$ for $M_a = 1$ and $\delta/R_a = 0.1$ for $M_a = 2$. For previously used nozzles ($D_a = 20$ mm), $\delta/R_a = 0.1$. Therefore, the new nozzles have hydraulically smoother inner surfaces than the old ones. Availability of nozzles with a high-quality inner surface allowed us to perform experiments on generation of controlled disturbances in the mixing layer in the form of steady streamwise vortices in order to study their topological structure and evolution in detail.

The following experimental technique was used. When a prescribed pressure P_0 was established in the plenum chamber of the nozzle and the Pitot tube position relative to the longitudinal axis was fixed, the dependences $P_t(r)$ were measured. Then, the dependences $P_t(\varphi)$ were measured with fixed values of the coordinates x and r. In the experiments with the jet unit of T-326, the pressure in the test chamber P_{ch} was different from the atmospheric value. Hence, a special system for controlling the pressure ratio P_0/P_{ch} directly in the course of the experiment was developed, which allowed sustaining this ratio at a constant level (in our case, $N_{pr} = P_0/P_{\text{ch}} = 5$).

The root-mean-square deviation of the total pressure registered in the plenum chamber from the mean value is approximately 1 %. Exhaustion of a supersonic underexpanded jet ($n_p = 2.64$) was obtained in the nozzle with $M_a = 1$, and the nozzle with $M_a = 2$ operated in the overexpansion mode ($n_p = 0.643$) ($n_p = P_a/P_{\text{ch}}$ is the jet pressure ratio and P_a is the pressure at the nozzle exit). The pressure ratio was constant in both cases: $N_{pr} = 5$. The jet Mach number determined by the formula for an isentropic flow

$$M_j = \sqrt{\frac{2}{\gamma - 1}\left[\left(\frac{P_0}{P_{\text{ch}}}\right)^{(\gamma-1)/\gamma} - 1\right]}$$

was sustained constant. In both exhaustion modes, we had $M_j = 1.71$.

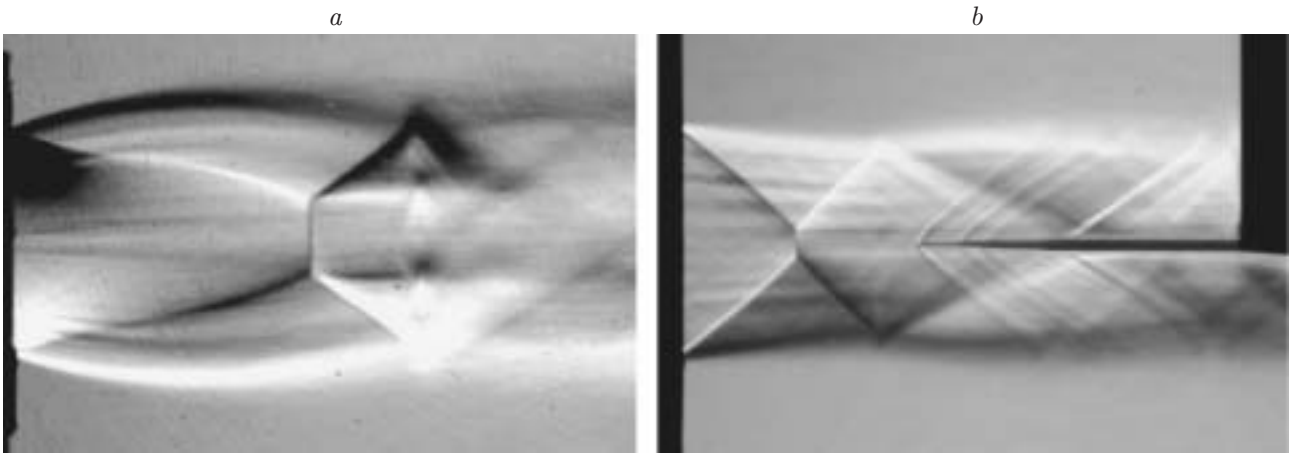

Fig. 3. Schlieren pictures of the jet for $M_a = 1$ (a) and 2 (b).

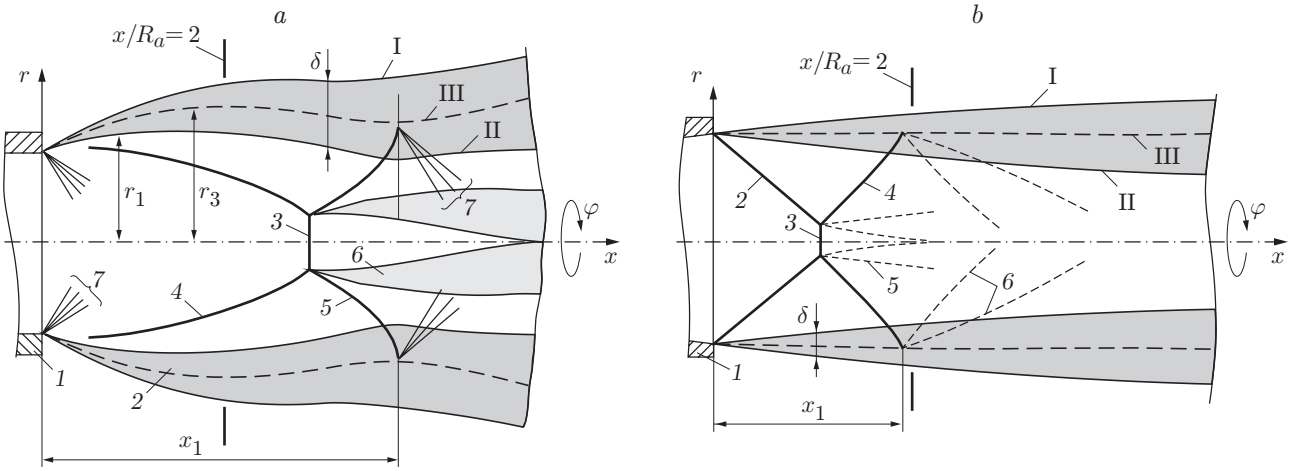

Fig. 4. Flow pattern on the initial part of the supersonic jet with $M_a = 1$ (a) and 2 (b): (a) 1) nozzle; 2) mixing layer (the outer and inner boundaries are indicated by I and II; the middle of the mixing layer is indicated by III; r_1 and r_3 are the radial distances corresponding to the inner boundary and to the middle of the mixing layer); 3) Mach disk; 4) barrel shock; 5) reflected shock; 6) shear layer formed behind the intersection point of shock waves 3, 4, and 5; 7) expansion fan; (b) 1) nozzle; 2) compression shock; 3) Mach disk; 4) reflected shock; 5) shear layer formed behind the intersection point of shock waves 2, 3, and 4; 6) expansion fan; the outer and inner boundaries of the mixing layer are indicated by I and II; the middle of the mixing layer is indicated by III.

The experiments were performed both for a smooth nozzle with natural roughness and for a nozzle with artificial microroughnesses on the inner surface. Each microroughness had a shape similar to that considered in [11], which was an isosceles triangle with an upstream-directed apex; this microroughness thickness was $k = 0.04$ mm (see Fig. 2). The microroughness elements were applied onto the inner surface of the nozzle near its exit section with an identical step in the azimuthal direction $\varphi = 45°$.

Figure 3 shows the schlieren pictures of the underexpanded jet ($n_p = 2.64$, $M_a = 1$, $Re_d = 2.21 \cdot 10^6$) and overexpanded jet ($n_p = 0.643$, $M_a = 2$, $Re_d = 1.95 \cdot 10^6$). The Reynolds number Re_d was based on flow parameters and nozzle-exit diameter. The flow direction was from left to right. The flow pattern was visualized by an IAB-451 shadowgraph by the schlieren technique with an inclined position of the sheet in the focal plane of the shadowgraph detector. The jets were exhausted from nozzles with microroughness elements glued onto the inner surfaces. The photographs were obtained with an exposure time of 0.1 msec. One can clearly see longitudinal fringes identified with streamwise vortex structures. The gas-dynamic structure of the initial part of the jet is characterized by the presence of shock waves, expansion waves, and a mixing layer. The flow patterns at the initial part of the supersonic jet with $M_a = 1$ and 2 are shown in Fig. 4. The length of the first barrel of the overexpanded jet ($x_1/R_a = 1.84$) is significantly smaller than the length of the first barrel of the underexpanded jet ($x_1/R_a = 3.75$).

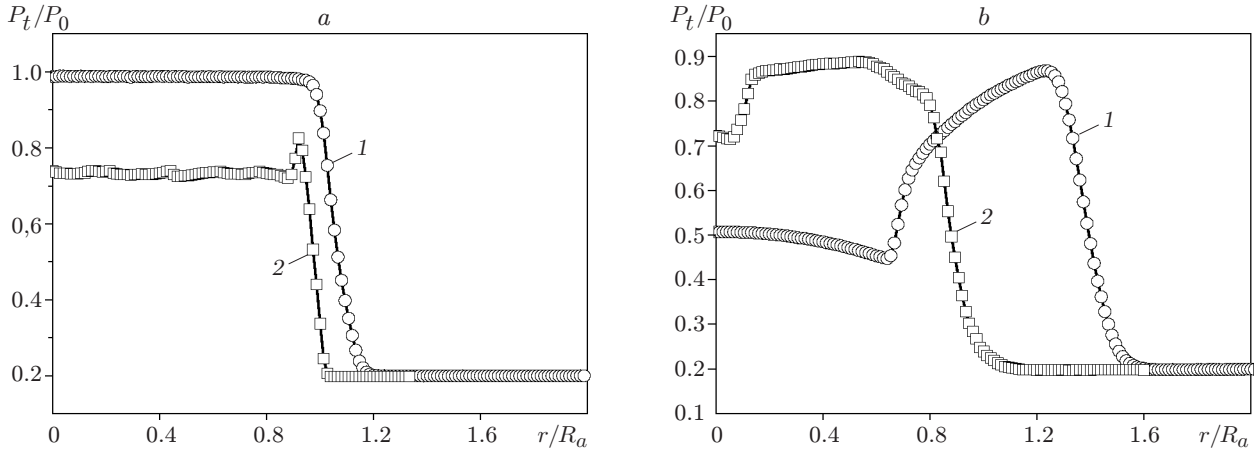

Fig. 5. Radial profiles of total pressure in supersonic jets for $x/R_a = 0.06$ (a) and 2.0 (b) and $M_a = 1$ (1) and 2 (2).

The gas-dynamic parameters of the jet flow were obtained by measuring the radial distributions of total pressure in different cross sections of the jet. The measurements were performed by a KPY43-A strain-gauge pressure probe produced by SIEMENS with a measurement range of 0–400 kPa. The following measurement technique was used. In a given cross section of the jet, the Pitot tube was mounted at the jet axis and then was moved by the traversing gear in the radial direction (discretely, with a step of 0.2 mm) toward the outer boundary; the pressure at this boundary corresponded to the pressure in the mixing chamber. The measurements were performed in the range $x/R_a = 0$–7 for jets exhausting from the convergent nozzle ($M_a = 1$) and from the Laval nozzle ($M_a = 2$).

The profiles $P_t(r)$ are plotted in Fig. 5. For $x/R_a = 0.06$, the pressure in the jet center, which was measured by the Pitot tube, was $P_t/P_0 = 0.987$ and 0.735 for $M_a = 1$ and 2, respectively. These values of P_t/P_0 correspond to flow Mach numbers $M = 1.23$ and 1.97 calculated by the Rayleigh formula. The value $M = 1.97$ is in good agreement with the geometric value of the flow Mach number at the exit of the Laval nozzle. For the convergent nozzle, the Mach number at the nozzle exit $M = 1.23$ differs from the design value $M = 1.0$. The reason is that the so-called boundary-layer bleeding is observed if an underexpanded jet is exhausted from the convergent nozzle [14]. This "bleeding" is understood as a decrease in boundary-layer thickness near the nozzle-exit section because of the favorable pressure gradient formed there by exhaustion of underexpanded supersonic jets. For this reason, the throat cross section corresponding to the flow Mach number $M = 1$ is shifted inside the nozzle, and a flow with the Mach number $M_a = 1.23$ is formed in the nozzle-exit section. This fact was noted in analyzing the flow structure at the initial part of a weakly underexpanded supersonic jet exhausting from a conical nozzle [15]. Calculations by formulas for an isentropic flow show that such a change in the Mach number corresponds to a 0.3-mm change in the boundary-layer displacement thickness in the nozzle-exit section, which indicates that the above-mentioned phenomenon is fairly realistic.

The total pressure profile 2 in the cross section $x/R_a = 0.06$ (Fig. 5a) for $M_a = 2$ has a small peak at the jet periphery ($r/R_a = 0.9$). The presence of this peak is explained by the change in the structure of shock waves interacting with the Pitot tube. A normal shock wave is formed in the jet core near the tip of the total pressure probe, and the shock near the Pitot tube tip interacts with the shock wave at $r/R_a = 0.9$ (see Fig. 3b). As a result of this interaction, the Pitot tube registers the total pressure behind a system of oblique shocks rather than the total pressure behind the normal shock. In the former case, the pressure registered by the probe is greater because of lower total pressure losses.

For $x/R_a = 0.06$, the size of the overexpanded jet is slightly smaller than that of the underexpanded jet (Fig. 5a). A more significant difference in transverse size is registered at $x/R_a = 2$, which is explained by compression of the overexpanded jet and expansion of the underexpanded jet (Fig. 5b). In the case of the underexpanded jet, a barrel shock is observed at $x/R_a = 2$ ($r/R_a = 0.65$), whereas reduced total pressure behind the Mach disk near the axis is registered in the overexpanded jet ($r/R_a = 0$–0.15). For $r/R_a = 1.25$, the Pitot tube registers the maximum pressure, which corresponds to the position of the inner boundary II of the mixing layer of the jet (see Fig. 4a).

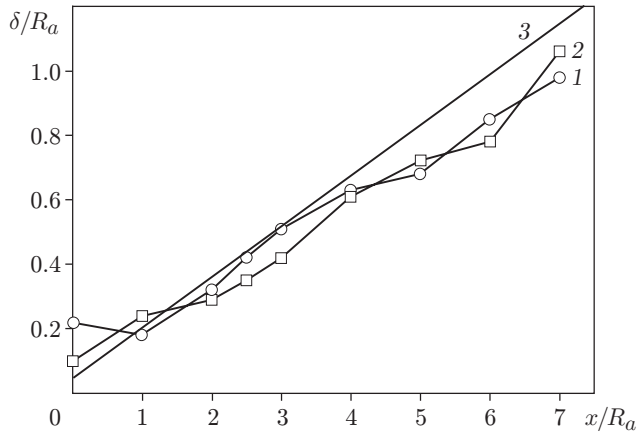

Fig. 6. Mixing-layer thickness versus the streamwise coordinate for two types of nozzles: $M_a = 1$ (1) and 2 (2); curve 3 is the approximation of experimental data [3].

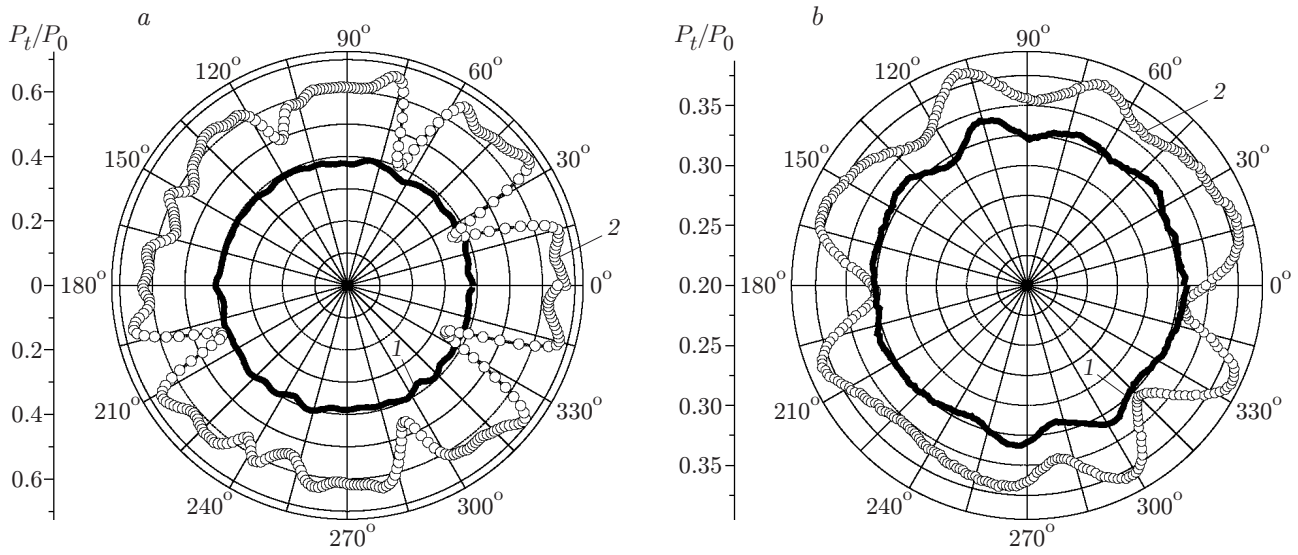

Fig. 7. Pressure distribution over the azimuthal angle (the concentric circles are the lines with an identical value of P_t/P_0) in the jet cross section $x/R_a = 2$: (a) $M_a = 1$, $r/R_a = 1.33$, and $k = 0.04$ mm; (b) $M_a = 2$, $r/R_a = 0.93$, and $k = 0.04$ mm; curves 1 and 2 show the data for the "smooth" nozzle and for the nozzle with microroughness elements, respectively.

An important parameter of the jet is the streamwise distribution of the mixing-layer thickness. The inner boundary of the mixing layer r_1 corresponds to the maximum of the function $P_t(r)$. The outer boundary of the layer r_2 is determined as a point where the pressure measured by the Pitot tube is $P_t(r_2) = 0.01P_t(r_1)$.

The mixing-layer thickness δ/R_a is plotted in Fig. 6 as a function of the streamwise coordinate x/R_a. The relative thickness of the mixing layer is determined by the formula $\delta = r_2 - r_1$, where r_1 and r_2 are the radii corresponding to positions of the inner and outer boundaries of the mixing layer.

It is seen in Fig. 6 that the character of the dependence $\delta(x)$ is approximately identical for the underexpanded and overexpanded jets. The greatest difference in the mixing-layer thickness is observed near the nozzle exit ($x/R_a = 0.06$), where the measured value of the mixing-layer thickness is close to the boundary-layer thickness near the nozzle exit.

The measurement results are in good agreement with data obtained previously for a convergent nozzle of radius $R_a = 20$ mm for $M_a = 1$ and $n_p = 2.65$ [3]. The insignificant difference in mixing-layer thickness confirms the governing role of the jet Mach number M_j equal to 1.7 in this particular case.

The azimuthal distributions of total pressure $P_t(\varphi)$ in the mixing layer of supersonic jets were measured in the nozzle without any additional disturbances on its inner surface and in the nozzle with artificial microroughness

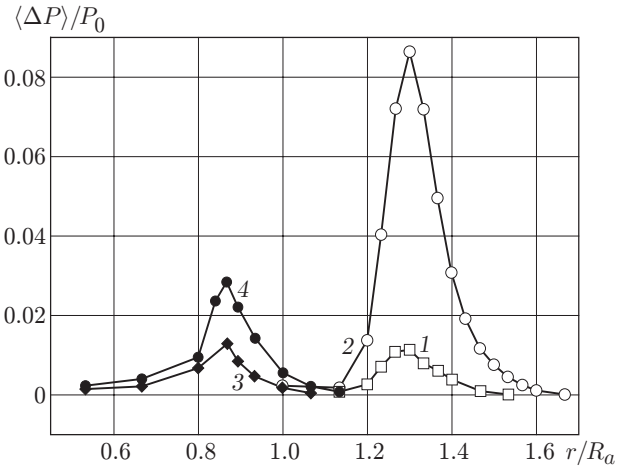

Fig. 8. Root-mean-square deviation of total pressure for $M_a = 1$ (1 and 2) and 2 (3 and 4).

TABLE 1

Number of the curve in Fig. 8	M_a	$n_p = P_a/P_{ch}$	M_j	$Re_d \cdot 10^{-6}$	K	$\langle\Delta P\rangle_{max}/P_0$	$K\|_{x/R_a=2}$
1	1	2.640	1.7	2.21	2.5	0.011	−0.085
2	1	2.640	1.7	2.21	40.0	0.086	−0.085
3	2	0.643	1.7	1.95	2.5	0.013	0.0005
4	2	0.643	1.7	1.95	40.0	0.028	0.0005

elements ("microtabs"). In the jet cross section $x/R_a = 2$ in the region of the mixing layer, 15–17 azimuthal dependences of the measured total pressure were obtained. Typical distributions are plotted in Fig. 7, which shows the experimental data obtained for a value of the jet radius r with the maximum variations in total pressure. For both types of the nozzle, the maximum variations are observed in the middle of the mixing layer. The plots clearly display the ordered character of the dependence $P_t(\varphi)$ caused by the presence of artificial microroughnesses on the inner surface of the nozzle. The maximum deviations of the azimuthal distribution of pressure in the mixing layer are observed for angles φ corresponding to positions of microroughness elements glued onto the inner surface of the nozzle.

The quantity $\langle\Delta P\rangle = \sqrt{(P_t^i - \bar{P})^2/(n-1)}$ characterizes the intensity of streamwise vortices in the mixing layer (P_t^i is the measured total pressure corresponding to the azimuthal angle φ_i, $\bar{P}$ is the mean value of pressure, and n is the number of measurements). The radial dependences of the relative root-mean-square deviation of total pressure $\langle\Delta P\rangle/P_0$ determined by azimuthal variations $P_t(\varphi)$ are shown in Fig. 8. The measurement results correspond to two gas-dynamic modes of exhaustion of the supersonic jet and two states of the inner surface of the nozzle. The main parameters of the jet are listed in Table 1.

In the case of natural roughnesses on the nozzle surface, the root-mean-square deviations of total pressure in the mixing layer $\langle\Delta P\rangle$ are almost identical (0.011–0.013) for the underexpanded and overexpanded jets (curves 1 and 3 in Fig. 8). In the presence of artificial microroughness elements on the inner surface of the nozzle (with a step of 45°), the level of disturbances in the mixing layer is different for the underexpanded and overexpanded jets. The maximum value for the overexpanded jet is $\langle\Delta P\rangle_{max}/P_0 = 0.028$ (curve 4), whereas this value reaches 0.086 for the underexpanded jet (curve 2).

For natural disturbances ($k \approx 0.0025$ mm), the level of disturbances in the mixing layers of both jets is approximately identical. The negative curvature of streamlines in the jet mixing layer leads to amplification of the Görtler disturbances for artificial perturbations ($k \approx 0.04$ mm). The character of transformation of disturbances generated by microroughness elements on the inner surface of the nozzle to steady azimuthal disturbances registered in the mixing layer depends also on the microroughness size. This indicates that there are threshold phenomena where the character of amplification of small perturbations differs from the character of amplification of high-amplitude disturbances. Such phenomena require a more careful study.

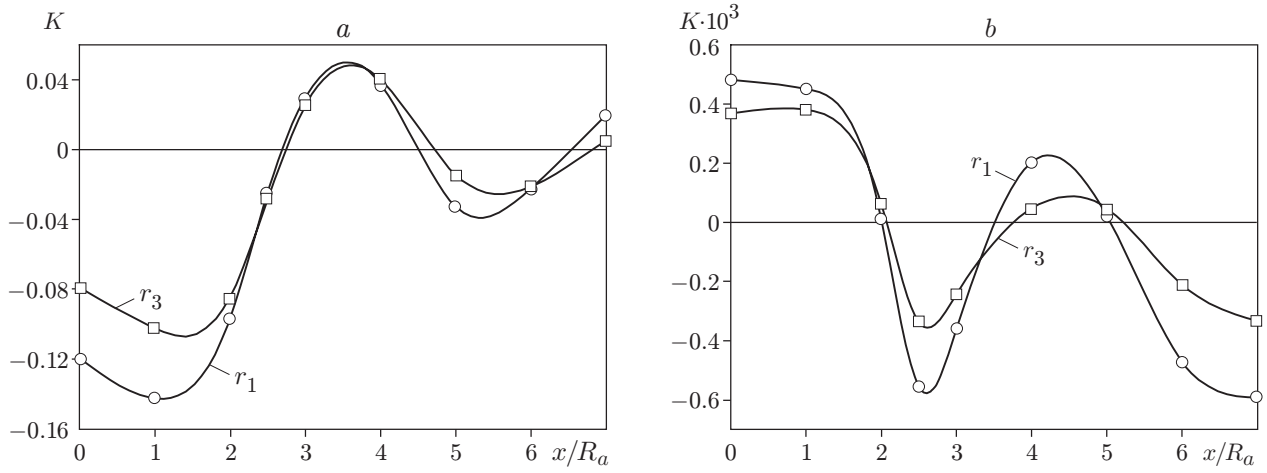

Fig. 9. Curvature of streamlines for two radial distances: $M_a = 1$ and $n_p = 2.64$ (a) and $M_a = 2$ and $n_p = 0.643$ (b).

A significant difference in the values of $\langle \Delta P \rangle_{\max}/P_0$ for jets with an identical jet Mach number and different jet pressure ratios can be explained by the difference in the geometric structure of the jets (see Figs. 3 and 4). The greatest difference is observed for the streamline curvature in the mixing layers of the jets. The maximum root-mean-square deviations are registered in the middle of the mixing layer both in the case of small (natural) roughnesses on the nozzle surface and in the presence of artificial microroughness elements.

The streamline curvature exerts the governing effect on development of the Görtler instability in supersonic jets. The curvature of a planar curve is calculated by the formula [16]

$$K = \frac{d^2y}{dx^2}\left[1 + \left(\frac{dy}{dx}\right)^2\right]^{-3/2},$$

where $y = y(x)$ is the dependence obtained by approximating experimental data. In this case, it is of interest to consider the curvature of the streamline corresponding to the middle of the mixing layer ($y \equiv r_3$). The experimental dependences for the inner boundary $r_1(x)$ and for the middle $r_3(x)$ of the mixing layer were obtained using the profiles $P_t(r)$ (see Fig. 5). The first and second derivatives of these dependences were obtained by a standard procedure of differentiation of the function defined by experimental points. The streamline curvature versus the streamwise distance is shown in Fig. 9a for a supersonic underexpanded jet and in Fig. 9b for an overexpanded jet. The streamline curvature for the middle of the mixing layer for $x/R_a = 2$ are listed in Table 1.

The curvature in the first cell is negative for the underexpanded jet and positive for the overexpanded jet. The pressure in the overexpanded jet is lower than the atmospheric value, and the jet flow is compressed by a shock wave. In the underexpanded mode, the atmospheric pressure is lower than the pressure in the flow at the nozzle exit; therefore, the jet is expanded when leaving the nozzle, and the curvature takes a negative value. In this case, the basic effect on curvature is exerted by the second derivative d^2y/dx^2; the term in the denominator $(dy/dx)^2$ is significantly lower than unity and, hence, has little effect on curvature. In the region of the first barrel, the maximum value of curvature for the underexpanded jet is observed in the first cell of the jet, which agrees with the data of [9, 15] for a supersonic jet exhausting from a conical nozzle ($M_a = 1$) with a diameter $D_a = 20$ mm.

In the case of the underexpanded jet, the curvature changes significantly in the fist cell of the jet. The same qualitative features are also typical of the overexpanded jet, but the maximum values of curvature are two orders lower than those in the underexpanded jet. The negative curvature of streamlines in the underexpanded jet and the positive curvature of streamlines in the overexpanded jet are the main specific features of the jet mixing layers under consideration. In accordance with the Rayleigh criterion, the disturbances in the curved shear layer are unstable and grow if $d\Gamma^2/dr < 0$ ($\Gamma = Vr$ is the circulation [17]). As applied to the flow considered, these conditions are satisfied at the initial part of the mixing layer of the supersonic underexpanded jet ($x/R_a < 2.75$), which was previously discussed in [7]. In this case, the flow velocity decreases with increasing radius, and the curvature has a negative value (similar to the flow past a convex surface). The experimental data show that the curvature at the initial part of the mixing layer in the overexpanded jet is very small and positive, which indicates that the Görtler instability is absent. Thus, for artificial disturbances, a significant increase in the level of variations of P_t in the

mixing layer of the underexpanded jet as compared to the overexpanded jet with the same value of the jet Mach number can be explained by the Görtler instability.

The study performed allowed us to develop a technique for generation of steady streamwise vortices in the mixing layer of supersonic jets by applying microroughness elements of controlled size onto the inner surface of the nozzle. The dependence of the mixing-layer thickness on the streamwise distance was obtained, and the propagation length for supersonic jets with $M_a = 1$ and 2 for an identical ratio of pressures $N_{pr} = 5$ and, hence, identical jet Mach number was determined. The mixing-layer thickness for both jets differs insignificantly, which indicates the governing influence of the jet Mach number on the character of mixing-layer evolution. A significant effect of microroughness elements of prescribed shape located on the nozzle surface on the registered variations of total pressure measured in the mixing layer of supersonic jets is revealed, as compared to the case of natural disturbances. The disturbance amplitude increases approximately by a factor of 8 for the underexpanded jet and by a factor of 3 for the overexpanded jet. The latter fact evidences a significant effect of streamline curvature on the character of evolution of streamwise vortices generated by artificial microroughnesses on the inner surface of the nozzle.

This work was supported by the Russian Foundation for Basic Research (Grant No. 02-01-00515) and by INTAS (Grant No. 99-0785).

REFERENCES

1. G. N. Abramovich, T. A. Girshovich, S. Yu. Krasheninnikov, et al., *Theory of Turbulent Jets* [in Russian], Nauka, Moscow (1984).
2. J. Schetz, *Injection and Mixing in Turbulent Flow*, Inst. of Aeronaut. and Astronaut., New York (1980).
3. E. J. Gutmark, K. S. Schadow, and K. A. Yu, "Mixing enhancement in supersonic free shear flows," *Annu. Rev. Fluid Mech.*, **27**, 375–417 (1995).
4. D. Liepman and M. Gharib, "The role of streamwise vortices in near-field entrainment of round jets," *J. Fluid Mech.*, **245**, 643–667 (1992).
5. V. I. Zapryagaev and A. V. Solotchin, "Spatial flow structure at the initial part of a supersonic underexpanded jet," Preprint No. 23-88, Inst. Theor. Appl. Mech., Sib. Div., Acad. of Sci. of the USSR, Novosibirsk (1988).
6. S. A. Novopashin and A. L. Perepelkin, "Axial symmetry loss of a supersonic preturbulent jet," *Phys. Lett.*, **135**, Nos. 4/5, 290–293 (1989).
7. V. I. Zapryagaev and A. V. Solotchin, "An experimental investigation of the nozzle roughness effect on streamwise vortices in a supersonic jet," *J. Appl. Mech. Tech. Phys.*, **38**, No. 1, 78–86 (1997).
8. V. I. Zapryagaev and A. V. Solotchin, "Evolution of streamwise vortices at the initial part of a supersonic nonisobaric jet in the presence of microroughnesses on the inner surface of the nozzle," *Izv. Ross. Akad. Nauk, Mekh. Zhidk. Gaza*, No. 3, 180–185 (1997).
9. V. N. Glaznev, V. I. Zapryagaev, V. N. Uskov, et al., *Jets and Unsteady Flows in Gas Dynamics* [in Russian], Izd. Sib. Otd. Ross. Akad. Nauk, Novosibirsk (2000).
10. D. C. MacCormic and J. C. Bennett (Jr.), "Vortical and turbulent structure of a lobed mixer free shear layer," *AIAA J.*, **32**, No. 9, 1852–1859 (1994).
11. A. Krothapalli, P. J. Strykowski, and C. J. King, "Origin of streamwise vortices in supersonic jets," *AIAA J.*, **36**, No. 5, 869–872 (1999).
12. V. I. Zapryagaev, "Streamwise vortices in a initial region of the supersonic nonisobaric jet shear layer," in: *Proc. of the Xth Int. Conf. on the Methods of Aerophysical Research* (Novosibirsk–Tomsk, July 9–16, 2000) [in Russian], Part 2, Izd. Sib. Otd. Ross. Akad. Nauk, Novosibirsk (2000), pp. 209–214.
13. V. I. Zapryagaev, N. P. Kiselev, and A. V. Solotchin, "Streamwise vortex structures at a boundary of the supersonic jet," in: *Proc. of the XI Int. Conf. on the Methods of Aerophysical Research* (Novosibirsk, July 1–7, 2002) [in Russian], Part 2, Nonparalel Publ., Novosibirsk (2002), pp. 192–196.
14. M. E. Deich, *Technical Gas-Dynamics* [in Russian], Énergiya, Moscow (1974).
15. V. I. Zapryagaev, A. V. Solotchin, and N. P. Kiselev, "Structure of a supersonic jet with varied geometry of the nozzle entrance," *J. Appl. Mech. Tech. Phys.*, **43**, No. 4, 538–543 (2002).
16. G. A. Korn and T. M. Korn, *Mathematical Handbook for Scientists and Engineers*, McGraw-Hill, New York (1961).
17. W. S. Saric, "Görtler vortices," *Annu. Rev. Fluid Mech.*, **26**, 379–409 (1994).